ORIGINAL ARTICLE

Brain-Targeted Delivery of Ropinirole by Mucoadhesive Intranasal Nanostructured Lipid Carriers for Parkinson's Disease Management

Vidhya Pravin Thorat, Avinash Ramrao Tekade

Department of Pharmaceutics, Marathwada Mitra Mandal's College of Pharmacy (Affiliated to Savitribai Phule, Pune University, Pune), Pune, Maharashtra, India

Abstract

Background: The therapeutic efficiency of orally delivered ropinirole (RP) is reduced due to extensive metabolic degradation during first-pass metabolism, resulting in moderate bioavailability and increased dosing frequency. To address these limitations, the present study aimed to prepare and evaluate mucoadhesive nanostructured lipid carriers (NLCs) of RP for intranasal (i.n.) administration to facilitate brain targeting. **Materials and Methods:** RP-NLCs were developed using the solvent diffusion method and optimized through a Box-Behnken design. Glyceryl monostearate and oleic acid were employed as lipid matrices, while Tween 20 and Pluronic F-68 functioned as surfactant and co-surfactant. **Results and Discussion:** The optimized formulation (RF13) exhibited a drug content of 98.12 ± 2.53% and entrapment efficiency of 95.18 ± 2.69%. The nanoparticles showed a mean particle size of 150.6 ± 2.13 nm, polydispersity index of 0.377 ± 0.14, and zeta potential of −33.8 ± 2.54 mV, indicating stable and uniform dispersion. *In vitro* studies demonstrated sustained drug release of 96.22 ± 3.25% over 4 h, while *ex vivo* permeation through goat nasal mucosa showed enhanced diffusion of 98.23 ± 2.25%. The addition of a mucoadhesive agent significantly improved detachment stress (6131.25 ± 1.22 dyne/cm^2) compared with the non-mucoadhesive system (3678.75 ± 3.24 dyne/cm^2). *In vivo* pharmacokinetic studies confirmed higher brain uptake with a C_{max} of 8.527 ± 0.54 µg/mL and plasma concentration of 1.876 ± 0.56 µg/mL at 1.5 h (T_{max}), supporting direct nose-to-brain transport. **Conclusion:** Findings of current research suggest that i.n. mucoadhesive RP-NLCs provide an effective delivery system for enhanced brain targeting, offering the potential to improve PD management while minimizing systemic adverse effects.

Key words: *Caesalpinia crista*, *in vivo*, intranasal, mucoadhesion, nanostructured lipid carriers, Parkinson's disease, pharmacokinetics study, ropinirole

INTRODUCTION

Parkinson's disease (PD) is becoming an increasingly growing burden on medical systems and the quality of patient life. Based on 2019 data from the World Health Organization, the global Parkinsonian syndrome population exceeded approximately 8.5 million individuals. This number represents a doubling in prevalence over the past 25 years, highlighting the growing impact of the disease on populations around the world. PD presents a significant global health challenge, contributing to approximately 5.8 million disability-adjusted life year in 2019, showing an 81% growth compared to 2000. The number of deaths attributed to PD also climbed significantly, reaching about 329,000, more than doubling since 2000. These figures underscore the growing impact of PD on both quality of life and mortality rates worldwide. In 2016, India was estimated to have nearly 0.58 million individuals living with PD, and a significant rise in prevalence is anticipated in the future. The central nervous system (CNS) presents considerable obstacles for medication delivery

Address for correspondence:
Dr. Avinash Ramrao Tekade, Department of Pharmaceutics, Marathwada Mitra Mandal's College of Pharmacy (Affiliated to Savitribai Phule, Pune University, Pune), Maharashtra, India.
Mobile: +91-9371152536.
E-mail: avitekade@gmail.com

Received: 26-10-2025
Revised: 18-01-2026
Accepted: 27-01-2026

because of the blood brain barrier (BBB), most therapeutic agents, including several neuroactive medicines, which limit the penetration into the brain parenchyma.[1] Therapies for PD and restless legs syndrome often include non-ergoline agents targeting D2 and D3 dopamine receptors; ropinirole (RP) hydrochloride is frequently utilized. Nonetheless, its oral administration is linked to significant first-pass metabolism and restricted bioavailability, which reduces its therapeutic effectiveness.[2,3]

Intranasal (i.n.) medication administration has become a promising option to circumvent the BBB and facilitate drug administration through the trigeminal and olfactory neuronal pathways facilitates brain targeting by a non-invasive route, resulting in rapid therapeutic onset, decreased systemic adverse effects, and increased patient compliance.[4,5] Conventional nasal formulations often experience fast mucociliary clearance, hence restricting drug residence duration and absorption.[6] To address this restriction, mucoadhesive nanoparticulate drug delivery devices have been thoroughly investigated. These devices may extend nasal residency duration, enhance medication absorption, and enable tailored delivery to the brain.[7] Nanoparticles formulated from biocompatible materials like chitosan, poly lactic-co-glycolic acid, and alginate have proven effective in improving the solubility, chemical stability, and absorption of CNS-directed therapeutics.

In this research, the primary aim is to prepare and characterize a mucoadhesive nanoparticulate technology that encapsulates RP for site-specific brain delivery through the i.n. pathway. This method is anticipated to augment cerebral bioavailability, diminish systemic adverse effects, and boost treatment results for individuals with PD.[8]

MATERIALS AND METHODS

Materials

RP given as a complimentary gift by USV Ltd. (Lote Parsuram) Ratnagiri. Gattefosse India Pvt. Ltd. (Mumbai, India) provided Gelucire 43/01and Glyceryl Monostearate (GMS). Oleic acid was purchased from New Neeta Chemicals, Pune. Loba Chemie provided castor oil, olive oil, Tween 80, and Poloxamer 188.

Selection of solid lipid (SL)

GMS, Compritol 888 ATO, Gelucire 43/01, and Precirol ATO 5 are SLs that were studied for their enhanced solubilization of RP. Each SL was heated to a temperature roughly 5°C higher than its melting temperature, after which the RP was gradually incorporated under gentle stirring to facilitate dissolution. Solubility was assessed visually, ensuring the complete absence of undissolved active pharmaceutical ingredients dispersed within the melted lipid. The lipid in which more drug is solubilized is selected for further formulation development.[9,10]

Selection of liquid lipid

Liquid lipids (2 mL) taken in separate microcentrifuge tubes, containing an excess amount (~10 mg) of RP, were added. Samples were vortexed and agitated at 25°C for 24 h by an Orbital shaker at 50 rpm (Labline, India) to allow equilibrium solubility to be reached. After centrifuging at 12,500 rpm for 30 min, the supernatant was passed through a 0.20 µm membrane filter to eliminate any remaining undissolved material. Ultraviolet (UV) spectroscopy at 247 nm was used to determine the concentration of RP in the filtrate after appropriate dilution with a suitable solvent.[11]

Selection of surfactants

Surfactants and cosurfactants were finalized based on their emulsion-forming efficiency with the selected lipid mixture. Several surfactants reported in the literature for their lipid-solubilizing capabilities were evaluated. To assess their performance, the lipid mixture dispersed in dichloromethane (DCM), followed by the addition of an aqueous surfactant solution (5% w/v) for each candidate surfactant. The formulations were maintained at 40°C for 10 min to ensure thorough evaporation of DCM. Subsequently, the diluted resultant formulation up to 10 mL of distilled water, and the percentage transmittance (%T) was determined at 510 nm using a UV-visible Spectroscopy (Jasco V-630, Model B206461148, Japan). Based on %T values, the surfactant having the greatest transmittance was designated as the main surfactant, and the next greatest value was assigned to be co-surfactant.[12]

Miscibility study of lipids

The miscibility of the chosen SL and LL in combination was assessed using the filter paper technique (lipid mix). Various lipid ratios (90:10, 80:20, 70:30, 60:40, and 50:50) were prepared utilizing a magnetic stirrer (Remi, 1 MLH, India) and heated at 70°C for 30 min, and subsequently cooling to prevailing temperature. The presence of oil droplets was assessed by spreading the lipid mixture onto filter paper. The ratio looked consistent with no oil droplets, and showed no indications of phase separation was chosen for this study.[13]

Extraction of mucoadhesive agent from *Caesalpinia crista*

Fresh mature seeds of the *C. crista* plant were collected from the Pune district, Maharashtra, India. The seeds were air-dried and coarsely ground using a grinder. A measured

quantity of 500 g of the seed powder was defatted using toluene and then subjected to 30 min. boiling with water. The emerging aqueous extract was filtered using a muslin cloth. To precipitate the semisolid mass, an excess of acetone was added. To purify the precipitate, it was rinsed with isopropyl alcohol. Finally, the purified material was freeze-dried for 24h at −60°C. Freeze-dried plant extract was collected, the percentage yield was calculated, and the extract was stored in a controlled environment until further use.[14]

Design of experiments (DOE) for RP-Nanostructured lipid carriers (NLCs)

The experimental design was developed employing Design-Expert® software (version 13; Stat-Ease Inc., Minneapolis, USA). A Box Behnken design (BBD) was applied to investigate the effects of independent variables [Table 1] on the particle size (PS), drug content (DC), entrapment efficiency (EE), and drug release (DR) as dependent parameters [Table 1]. 17 experimental runs were carried out using a BBD, with 5 center point repetitions included to examine reproducibility and stability at the midpoint of the factor ranges.

Formulation of RP-NLCs

The solvent diffusion method was used to prepare NLCs using oleic acid (LL) and GMS (SL) as outlined in Table 2. In brief, the weighed amounts of GMS, oleic acid, and RP were solubilized in 10 mL of a 1:1 (v/v) ethanol-acetone mixture, followed by heating in a water bath at 55°C. An aqueous solution containing Poloxamer 188 and Tween 20 (each 1% w/v) at room temperature was stirred with continuous addition of the organic phase to form the NLC suspension. A mucoadhesive agent (0.5%) was incorporated during the stirring process.[15-17]

Optimization of dependent variables

RP-NLC was optimized with the help of A BBD, aimed to assess effects of three independent variables – lipid concentration (3–5% w/w, X_1), surfactant concentration (3–5% w/w, X_2), and stirring speed (1000–1200 rpm, X_3), on four dependent responses: PS (Y_1), DC (Y_2), EE, (Y_3), and (DR, Y_4). The experimental data were analysed using a DOE approach to generate predicted values, polynomial regression equations, and 3D surface response plots. The relationship between independent variables and responses was examined, and the optimal regression model (linear, quadratic, or 2FI) was chosen using analysis of variance (ANOVA) and fit statistics (R^2, adjusted R^2, and predicted R^2) at a significance level of $P < 0.05$. Model validation involved calculating the prediction error (%) for the most desirable formulation.

Table 1: Factors and the corresponding levels for the development of ropinirole-loaded nanostructured lipid carriers

Independent variables (%)	Low	Middle	High
X_1: Lipid conc.	3	4	5
X_2: Surfactant conc.	3	4	5
X_3: Stirring speed (rpm)	1000	1100	1200
Dependent variables (%)	**Constraints**		
Y_1: PS (nm)	Minimize		
Y_2: DC	Maximum		
Y_3: EE	Maximum		
Y_4: DR	Maximum		

PS: Particle size, DC: Drug content, DR: Drug release, EE: Entrapment efficiency

Table 2: Experimental batches of ropinirole NLCs

Runs	X_1: Lipid conc. (%)	X_2: Surfactant conc. (%)	X_3: Stirring speed (rpm)
RF1	4	4	1100
RF2	3	3	1100
RF3	4	5	1200
RF4	3	4	1000
RF5	4	4	1100
RF6	4	3	1200
RF7	5	4	1000
RF8	4	4	1100
RF9	3	5	1100
RF10	5	4	1200
RF11	5	3	1100
RF12	4	5	1000
RF13	4	4	1100
RF14	4	4	1100
RF15	5	5	1100
RF16	4	3	1000
RF17	3	4	1200

NLCs: Nanostructured lipid carriers

Characterization of RP-NLCs

PS, polydispersity index (PDI), and zeta potential (ZP)

An aliquot of the RP-NLC suspension was diluted with distilled water and subjected to sonication for 30 min before analysis; the procedure was carried out under controlled conditions at 25°C. Formulations were evaluated using the dynamic light scattering technique (SZ-100 Zetasizer, Horiba Scientific, Japan). The mean PS (Z-average) and PDI were analysed using disposable polystyrene cuvettes (DTS0012) at 25°C with a fixed 90° side-scattering angle. Surface charge and colloidal stability were assessed through ZP measurements using a Dip Cell (ZEN1002)

attached to the same instrument, following a similar dilution protocol.[18-20]

DC

The RP-NLC suspension (1 mL) was diluted with methanol, followed by sonication for 15 min to ensure full solubilization of the drug. UV–visible spectrophotometric analysis (Jasco V-630, Model B206461148, Japan) was employed to record the absorbance of the prepared solution at a wavelength of 247 nm. The DC was then calculated using the appropriate formula, Equation 1.[21-23]

$$DC(\%) = \frac{\text{Drug amount in the formulation}}{\text{Drug amount theoretically added}} \times 100 \quad (1)$$

EE

RP-NLC (3 mL) was loaded into an ultrafiltration centrifuge tube and subjected to elutriation at 4,000 rpm for 20 min at 4°C using an ultracentrifuge (Optima MAX-XP, Beckman Coulter, USA) to distinguish unencapsulated drug from nanoparticle-bound drug. The supernatant containing unencapsulated drug carefully withdrawn, filtered from a 0.22 µm membrane filter, and analyzed for wavelength 247 nm utilizing a UV–Visible spectrophotometer. The EE subsequently calculated using Equation 2.[24,25]

$$EE(\%) = \frac{\text{Total drug added} - \text{Drug in supernatant}}{\text{Total drug added}} \times 100 \quad (2)$$

In vitro release study

In vitro release studies of RP-loaded NLC were conducted at 37°C using phosphate buffer (pH 6.4) as the release medium. A precisely measured 2 mL of the RP-loaded NLC formulation was transferred to a dialysis membrane, ensuring that the formulation made contact with the membrane surface. The membrane was then immersed in 100 mL of pH 6.4, which served as the receiving medium. The receiving compartment was kept on a magnetic stirrer set at 75 rpm (Remi) and maintained at 37°C. At specified intervals (1, 2, 3, and 4 h), 5 mL samples were withdrawn from the receiving compartment. The released amount of RP was quantified using a spectrophotometer set at 247 nm (Jasco V-630). After each sample withdrawal, an equivalent volume of pH 6.4 was added back to the receiving compartment to maintain the system's volume.[26-28]

Morphological evaluation

Transmission electron microscopy (JEOL 2200FS, Japan) was utilized to examine the surface morphology of the optimized RP-NLC. A few microliters of optimized batch were laid onto a 300-mesh copper grid covered using carbon film, which was used and then allowed for air drying. Following drying, the sample was treated with a 2% w/v phosphotungstic acid solution, and additional stain gently wiped using filter paper. Morphological analysis, along with image acquisition, was performed using Digital Micrograph and Soft Imaging Viewer software.[29]

Mucoadhesive strength (MS) determination

The Wilhelmy plate method is used to determine surface or interfacial tension at the boundary between air and liquid or between two immiscible liquids under equilibrium conditions. Vials with rubber closure were coated with standard and test mucoadhesive agent by dipping into a 3 mL solution. Nasal mucosa was excised from sheep and placed in an appropriate container, maintaining the temperature at 37 ± 0.5°C throughout the experiment. A thread was tied to one end of the vials, while the setup allowed for weights to be added to the opposite end. Vials were gradually removed from the surface of the nasal mucosa by applying successive weights at predetermined times, and the detachment force from the mucin layer was quantified under standardized conditions.[27]

The force in Newton's (NF) was calculated by Equation 3:

$$NF = \frac{0.00981\ W}{2} \quad (3)$$

Here, "W" represents the weight of water used in the experiment. A custom-designed (locally fabricated) apparatus was utilized to measure the minimum force needed to separate two membranes with a layer of gel applied between them. This setup was employed to determine the least amount of water weight necessary to remove the test sample through the sheep nasal mucosa. The MS, expressed as detach force (dyne/cm^2), was calculated according to Equation 4.

$$MS = \frac{m \times g}{A} \times 100 \quad (4)$$

Where "m" represents the weight (in g) required to achieve separation of the membrane from the underlying tissue. The term "g" denotes the acceleration due to gravity, which is standardized at 980 cm/s^2. Surface area "A" (in cm^2) of the exposed mucosal membrane involved in the experimental setup.[27]

Ex vivo permeability study

Ex vivo permeation analysis performed utilizing phosphate-buffered saline (PBS) (pH 6.4) with the help of fixed-dose combination. In between the donor and receptor compartments, freshly isolated, excised sheep nasal mucosa was carefully mounted, ensuring the mucosal side faced the receptor chamber. An aliquot of 0.5 mL of the analyzing formulation was introduced into the donor chamber. The setup was kept at 37 ± 0.5°C under constant magnetic stirring at 100 rpm, and receptor chamber samples were collected at scheduled intervals over a 4-h period while maintaining sink conditions. A UV-Visible spectrophotometer at 247 nm was used for the determination of the amount of drug

permeated.[30,31]

In vivo pharmacokinetic study

Twenty-four healthy albino Wistar rats weighing 200 and 250 g were used. On arrival, the animals were acclimatized and housed under standardized lab conditions, ensuring a consistent ambient temperature of 25 ± 5°C and a 12 h light/dark cycle. Rats were acclimated for a designated period, with unlimited access to drinking water and standard pellet feed. The study comprised two groups, with each group consisting of twelve animals. Based on previous pharmacokinetic and tissue distribution studies, the sample size was determined, ensuring sufficient statistical power to detect significant differences between groups while accounting for potential biological variability and sample loss.

After induction of anesthesia and sacrifice, blood and brain samples were collected at scheduled intervals. Blood (2 mL) was obtained through cardiac puncture into ethylenediaminetetraacetic acid tubes and maintained under refrigerated conditions until processing. Plasma was isolated by elutriation at 5,000 rpm till 15 min. For sample preparation, plasma was treated with an internal standard and deproteinized using acetonitrile (2 mL), followed by vortexing and elutriation at 4,000 rpm till 5 min. The clear supernatant separated, dried at ambient temperature, reconstituted in the mobile phase, and membrane-filtered (0.22 µm) before analysis.

Immediately, once blood was collected, the animals were humanely euthanized by decapitation, and the skull was carefully opened to extract the brain. The excised brain tissues were rinsed with isotonic saline to remove any adherent blood, blotted dry using filter paper, and stored in PBS. Brain tissues were homogenized employing a tissue homogenizer for 1 min. at 10,000 rpm, followed by centrifugation for separation of supernatant. Both plasma and brain samples were analysed utilizing validated high-performance liquid chromatography method for quantification of RP.[4]

Statistical analysis

Statistical equivalence among experimental groups was performed by GraphPad Prism version 10.0. Data are recorded as mean ± standard deviation (SD), with significance accepted at $P < 0.05$. SD represented by error bars in all graphs to ensure an accurate and consistent interpretation of data variability.

RESULTS AND DISCUSSION

Selection of lipids and surfactants

The solubility of RP in various SLs and LLs was assessed as part of the lipid screening process for the NLC formulation. GMS (75.40 ± 2.45 mg/g) and oleic acid (48.91 ± 1.12 mg/mL) exhibited the highest solubility among SLs and LLs, respectively, and were thus selected. The emulsification efficiency of various surfactants with lipid mixtures was assessed using %T as an indicator of clarity and dispersion stability. Among the tested surfactants, Tween 20 exhibited the highest %T of 97.56 ± 1.25%, reflecting its superior emulsification ability with the lipid system. Poloxamer 188 also showed a relatively high %T of 95.48 ± 1.86%.

Miscibility study

Compatibility between GMS and oleic acid at different proportions was investigated with a smear test. SLs and LLs mixtures were spread on filter paper and monitored for phase separation. The blend of GMS and oleic acid in a 70:30 ratio stayed clear and showed no phase separation for up to 48 h, while preserving a solid-to-semisolid texture at room temperature. The presence of LLs within the SLs matrix induces crystal imperfections, facilitating higher drug incorporation and reducing the potential for drug leakage.[13]

Identification tests of *C. crista* seed extract

The Molisch, Ninhydrin, Biuret, and Salkowski tests confirmed the appearance of carbohydrates, amino acids, proteins, and terpenoids, respectively, in the *C. crista* seed extract following extraction. The Molisch test indicated a positive result with a violet ring at the interface, confirming carbohydrates. In contrast, the Ninhydrin test turned the colorless solution blue, confirming amino acids, and the Salkowski Test reddish brown color at the interface, indicating terpenoids.[32-34]

Optimization of formulation

Influence of process variables on PS (Y_1)

ANOVA for PS reveals the model is statistically significant (F-value = 3.65, $P = 0.0348$), implying that the experimental parameters meaningfully affect PS. The mechanical stirrer speed (C) is the only individual term with a significant effect ($P = 0.0142$), indicating that it plays a major role in controlling PS (Equation 5). Since the lack of fit is not statistically significant ($P = 0.1281$), it suggests that the model adequately represents the experimental data, with residual variation largely attributed to random error rather than inadequacy of the model. The model demonstrated an $R^2 = 0.6866$, accounting for 68.66% of the variation in PS. The similarity between adjusted R^2 (0.4986) and predicted R^2 (0.4985) indicates reasonable predictive performance. An adequate precision value of 6.6143 further supports the suitability of the model by confirming an acceptable signal-to-noise ratio [Figure 1a and b].

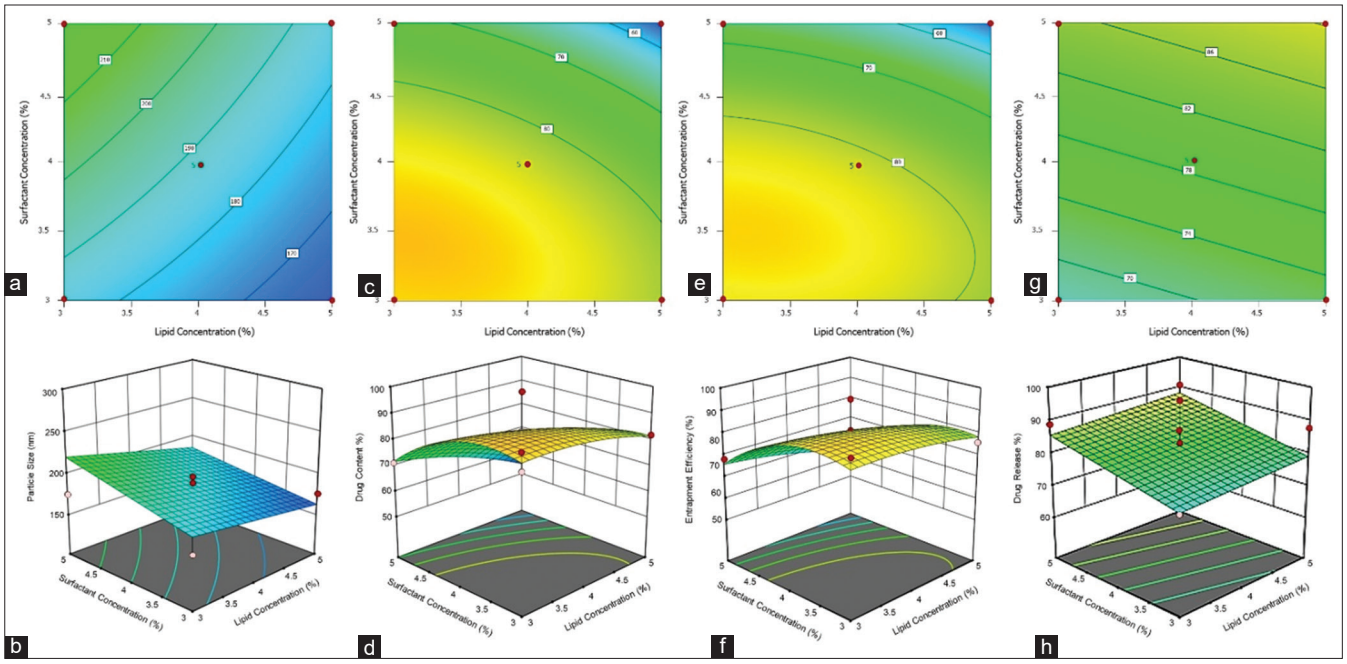

Figure 1: 4D-contour and 3D-surface plots depicting the interactive effects of surfactant concentration and lipid concentration on key nanocarrier characteristics: Particle size (a and b), drug content (c and d), entrapment efficiency (e and f), and drug release (g and h)

$$Y1 = 188.06 - 14.21A + 14.56B + 28.83C - 3.50AB - 29.58AC + 27.78BC \quad (5)$$

Influence of process variables on DC (Y_2)

The ANOVA analysis for DC revealed that the overall quadratic model is significant, with an F-value of 4.34 and a $P = 0.0330$, suggesting that the final formulation and processing factors collectively have a strong influence on DC. Among the individual factors, surfactant concentration (B) is significant ($P = 0.0049$), which implies a strong effect on DC. The interaction between surfactant concentration and mechanical stirrer speed (BC) is also significant ($P = 0.0241$), highlighting a synergistic effect between these two parameters (Equation 6).

$$Y2 = 83.74 - 5.88A - 10.77B + 3.75C - 2.78AB - 0.0775AC + 10.78BC - 2.49A^2 - 7.44B^2 + 6.07C^2 \quad (6)$$

Other factors, such as lipid concentration (A), mechanical stirrer speed (C), and their squared terms (A^2, B^2, and C^2), while not statistically significant at $P < 0.05$, may still positively influence the robustness of the model and are often retained to preserve hierarchical structure. The absence of a significant lack of fit ($P = 0.8008$) suggests that the model satisfactorily describes the experimental observations, with most unexplained variation arising from random error. A relatively high $R^2 = 0.85$ explains about 85% of the variation for DC. The difference between adjusted R^2 (0.6524) and predicted R^2 (0.3193) suggests moderate predictive performance, highlighting potential scope for further model refinement. The adequate precision of 7.9331 confirms an acceptable signal-to-noise ratio [Figure 1c and d].

The non-significant lack of fit ($P = 0.8008$) indicates that the model satisfactorily describes the experimental observations, with most unexplained variation arising from random error. The model exhibits a comparatively high coefficient of determination (COD) ($R^2 = 0.85$), demonstrating that approximately 85% of the variation in DC is accounted for. The disparity between the adjusted R^2 (0.6524) and predicted R^2 (0.3193) reflects moderate predictive capability, suggesting opportunities for further improvement of the model. In addition, an adequate precision value of 7.9331 confirms a sufficient signal-to-noise ratio.

Influence of process variables on EE (Y_3)

The ANOVA analysis for EE explains *F*-value of 4.06 indicates the model is significant, and a corresponding $P = 0.0391$. This suggests that final formulation and process variables exert a significant influence on EE. Among the model terms, surfactant concentration (B) has a particularly strong effect, with a $P = 0.0072$, highlighting its high statistical significance. In addition, the interaction between surfactant concentration and mechanical stirrer speed (BC) is significant ($P = 0.0311$), indicating a meaningful synergistic effect on EE.

Although individual terms such as lipid concentration (A) and mechanical stirrer speed (C) at the 0.05 level are not statistically significant, they may still contribute to the overall model's predictive ability and are typically retained to maintain model hierarchy. The squared terms B^2 ($P = 0.0534$) and C^2 ($P = 0.0820$) are close to significance, suggesting potential curvature in the response surface that may warrant further investigation. The lack-of-fit analysis shows no statistical significance ($P = 0.7207$), confirming that the

model adequately fits the experimental values and that the remaining variability is primarily due to random error rather than systematic deviations. The COD (R^2 = 0.8392) suggests that Equation 7 accounts for nearly 84% of the variation in EE. However, the noticeable between the adjusted R^2 (0.6325) and predicted R^2 (0.1458) points to limited predictive strength, implying that further refinement of the model, possibly by incorporating additional influential variables, may be necessary. The appropriate precision value of 7.0501 reflects an acceptable signal-to-noise ratio, supporting the model's suitability for design space exploration [Figure 1e and f].

$$Y3 = 81.26 - 4.51A - 10.71B + 5.06C - 1.97AB + 1.34AC + 10.88BC - 2.02A^2 - 9.14B^2 + 8.00C^2 \quad (7)$$

Influence of process variables on DR (Y_4)

ANOVA of DR revealed a significant linear model, having an F-value of 3.70 and a P = 0.0402, this implies the formulation and processing factors jointly exert a significant influence on DR. From the individual variables, mechanical stirrer speed (C) implies a statistically significant effect (P = 0.0208), underscoring its strong influence on the release rate. Although surfactant concentration and lipid concentration are not statistically significant (P = 0.5908 and 0.0707, respectively), surfactant concentration approaches the significance threshold and may still contribute to the response.

The non-significant lack-of-fit result (P = 0.9315) analyses that the model provides an appropriate description of the experimental values, with the remaining variation largely attributable to random error rather than systematic bias. The COD (R^2 = 0.4604) indicates that approximately 46.04% of the variation for DR is captured by the model. The close alignment between the adjusted R^2 (0.3358) and predicted R^2 (0.3256) demonstrates acceptable model consistency and moderate predictive performance (Equation 8). In addition, the adequate precision value of 6.7018, which exceeds the recommended threshold of 4, results a satisfactory signal-to-noise ratio and supports the model's suitability for design space optimization [Figure 1g and h].

$$Y4 = 82.38 + 1.25A + 4.48B + 5.99C \quad (8)$$

Characterization of optimized RP-NLCs

RP-NLC formulations were prepared, and RF-13 was selected as the optimized batch because it demonstrated the most desirable combination of critical parameters among all the formulations tested. Specifically, it exhibited the smallest PS along with a narrow size PDI, indicating efficient nanoformulation and uniformity. In addition, its high ZP suggested robust colloidal stability, essential for preventing aggregation. These qualities collectively identify formulation 13 as the most promising candidate for further characterization and in-depth evaluation.

PS, PDI, and ZP

The characterization of RP-NLCs revealed that PS of prepared batches ranged from 150.6 ± 2.13 to 292.2 ± 1.46 nm, having

Table 3: Observed responses of prepared RP-NLC batches

Run	PS (nm)	PDI	ZP (mV)	EE (%)	DC (%)	DR (%)
RF1	189.6±1.28	0.372±0.12	−35.1±2.42	69.33±1.25	73.76±2.56	71.67±1.24
RF2	164.8±2.12	0.370±0.11	−35.6±1.45	88.20±2.56	91.25±1.58	76.34±1.19
RF3	284.4±1.24	0.335±0.14	−35.6±2.58	86.22±1.12	90.01±2.10	87.63±2.53
RF4	174.5±2.25	0.429±0.10	−34.8±1.89	84.05±2.58	89.68±2.60	72.99±1.18
RF5	178.5±1.24	0.295±0.03	−34.1±2.43	79.62±3.25	80.79±1.58	83.09±1.56
RF6	174.5±2.36	0.429±0.16	−33.5±1.48	83.45±1.58	85.98±2.23	81.42±1.96
RF7	171.8±1.85	0.342±0.18	−32.7±1.89	79.62±2.59	81.22±1.89	70.29±1.24
RF8	197.2±2.47	0.401±0.03	−36.3±3.25	80.75±2.03	82.66±2.10	87.26±1.88
RF9	175.3±1.22	0.326±0.17	−36.5±1.23	68.30±1.58	71.28±1.87	88.95±2.84
RF10	171.2±1.56	0.403±0.08	−35.3±1.02	93.11±3.59	84.81±2.43	86.34±1.24
RF11	176.7±2.58	0.233±0.06	−29.8±2.56	75.83±2.53	81.91±2.65	87.70±1.63
RF12	171.5±2.43	0.375±0.07	−33.6±3.89	55.02±2.47	57.19±3.54	82.53±2.48
RF13	150.6±2.13	0.377±0.14	−33.8±2.54	95.18±2.69	98.12±2.53	96.22±3.25
RF14	180.8±1.87	0.361±0.16	−34.2±2.01	81.40±3.65	83.37±3.59	82.23±2.58
RF15	173.3±1.36	0.392±0.18	−34.7±1.82	48.04±2.87	50.81±2.48	90.16±3.56
RF16	173.1±1.86	0.219±0.10	−28.7±3.02	95.76±1.48	96.29±3.89	80.45±2.47
RF17	292.2±1.46	0.319±0.18	−32.2±1.14	92.16±3.26	93.58±2.43	68.45±3.58

PDI: Polydispersity index, ZP: Zeta potential, EE: Entrapment efficiency DC: Drug content, DR: Drug release, PS: Particle size, RP-NLC: Ropinirole-nanostructured lipid carriers

PDI values among 0.219 ± 0.10 and 0.429 ± 0.16, indicating uniform and stable nanoscale formulations [Table 3]. ZP measurements varied from −36.5 ± 1.23 to −29.8 ± 2.56 mV, reflecting sufficient surface charge to ensure colloidal stability and prevent aggregation. The optimized formulation (RF13) demonstrated the smallest PS (150.6 ± 2.13 nm), acceptable PDI (0.377 ± 0.14), and high ZP (−33.8 ± 2.54 mV), highlighting its superior physical stability, uniformity, and suitability for enhanced drug delivery. Collectively, these results confirm effective nanoparticle engineering with promising implications for improved bioavailability and therapeutic efficacy.

DC and EE

The DC and EE of the prepared RP-NLC batches exhibited values ranging from 50.81 ± 2.48% to 98.12 ± 2.53% and 48.04 ± 2.87% to 95.76 ± 1.48%, respectively, demonstrating efficient drug incorporation within the lipid matrix [Table 3]. The optimized formulation (RF13) showed the highest EE of 95.18 ± 2.69% and DC of 98.12 ± 2.53%, indicating superior capacity for drug loading. These high values suggest an effective lipid matrix with an imperfect crystalline structure that facilitates better drug accommodation and minimizes leakage. Overall, the results highlight the formulation's potential for delivering a therapeutic payload with enhanced stability and sustained release characteristics.

In vitro release study

The DR from the various RP-NLC batches ranged from 68.45 ± 3.48% to 96.22 ± 3.25% at the end of 4 h, indicating substantial variability based on formulation parameters [Table 3]. Notably, the optimized batch (RF13), comprising 4% lipid, 4% surfactant, and a stirring speed of 1200 rpm, achieved the highest DR (96.22 ± 3.25%), illustrating an effective balance between matrix composition and process conditions. Increased surfactant content and higher stirring speeds promoted improved encapsulation and dispersion, which enhanced drug diffusion from the carrier. These findings confirm that the systematic variation in lipid and surfactant concentrations, along with stirring speed as outlined in the BBD, directly influences the release profile, ultimately enabling superior controlled delivery for the optimized formulation [Figure 2a and b].[27]

Ex vivo permeation study

Among all the formulations (RF11–RF17), RF13 demonstrated the most effective DR profile, reaching 98.23 ± 2.25% at 4 h, the highest among all tested batches [Figure 2c and d]. It showed a rapid and consistent release rate across each time point, indicating excellent formulation characteristics such as optimal polymer concentration, uniform PS, and EE. The

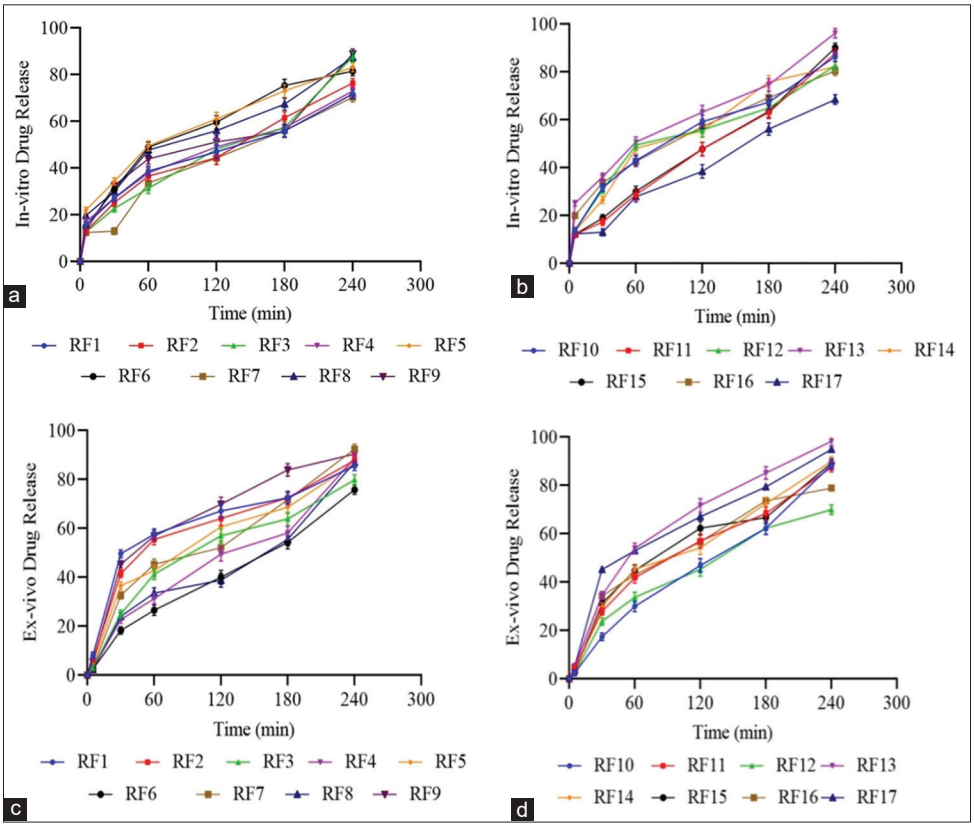

Figure 2: Comparative drug release study, *in vitro* drug release (a and b) using dialysis method, and *ex vivo* (c and d) using goat nasal mucosa in phosphate-buffered saline phosphate buffer at 37 ± 0.5°C for 5 h. Data are stated as mean ± standard deviation (n = 3)

Table 4: Pharmacokinetic parameters of RP-NLC

Parameters	Brain tissues		Blood plasma	
	i.v. solution	i.n. NLCs	i.v. solution	i.n. NLCs
C_{max} (µg/mL)	3.055±0.98	8.527±0.56	12.854±0.32	1.876±0.56
T_{max} (h)	1.5	1.5	00	1.5
AUC $_{o\text{-}5.5}$ (µg/µL×h)	0.007639	0.0209343	0.0325714	0.003832
$t_{1/2}$ (h)	1.19528	0.50158	0.908176	0.835258

*i.v.: Intravenous, i.n.: Intranasal, RP-NLCs: Ropinirole-nanostructured lipid carriers, AUC: Area under the curve

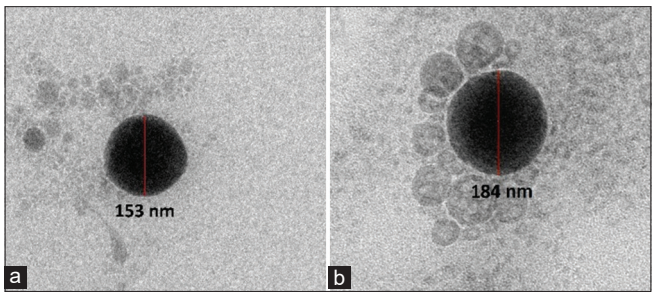

Figure 3: (a and b) Morphological evaluation of optimized nanostructured lipid carrier (RF13)

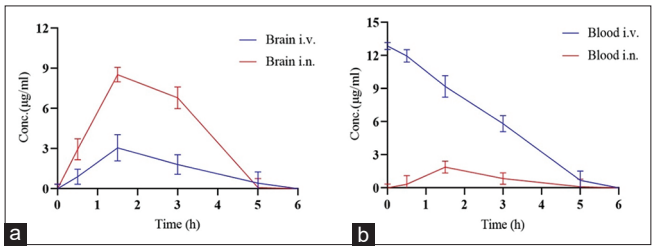

Figure 4: Pharmacokinetic concentration–time profiles of ropinirole-nanostructured lipid carriers in brain tissue following intranasal (i.n.) and intravenous (i.v.) administration (a), and corresponding plasma concentration–time profiles after i.n. and i.v. administration (b)

performance of RF13 suggests its strong potential as the lead candidate for sustained and effective drug delivery, making it highly suitable for further development and scale-up.[31]

Morphological evaluation

The analysis of the optimized Batch (RF13) provides evidence of spherical nanoparticles exhibiting well-defined and uniform morphology. The particles are distinctly separated with negligible aggregation, indicating favorable colloidal stability. A representative nanoparticle displays a size of approximately 152.6 nm, consistent with the desired nanoscale dimensions for efficient drug delivery [Figure 3]. The homogeneity in shape and size supports effective drug encapsulation and suggests improved permeation and cellular internalization, correlating with the enhanced *in vitro* DR performance observed for RF13.

Mucoadhesion force by Wihelmy's method

The mucoadhesion study reveals that RF13 exhibits significantly stronger adhesion compared to RF (without a mucoadhesive agent). RF13 demonstrates a higher detachment stress (6131.25 ± 1.22% dyne/cm^2) and force (0.122 N), requiring more effort for detachment, indicating enhanced mucoadhesive properties. In contrast, RF, lacking a mucoadhesive agent, shows lower detachment stress (3678.25 ± 3.24% dyne/cm^2) and force (0.0735 N), suggesting weaker adhesion and easier detachment. Thus, RF13 is considered an optimized batch for applications requiring strong mucoadhesion, ensuring prolonged retention and sustained drug delivery.

In vivo pharmacokinetic study

IN RP-NLC and RP intravenous (i.v.) solution pharmacokinetic profiles are shown in Figure 4a and b. This data shows that RP was more in the brain than in the plasma, indicating the brain targeting of the NLCs. Table 4 indicates C_{max} 8.527 ± 0.54µg/mL and area under the curve (AUC) of i.n. NLC (0.0209 µg/µL × min) significantly improved ($P < 0.05$) as compared with the C_{max} (3.055 ± 0.98 µg/mL) and AUC (0.00764 µg/µL × min) of i.v. RP solution in the brain tissues. Similarly, the t_{max} was significantly augmented after incorporation of the drug in the RP-NLCs (1.5 h).

CONCLUSION

RP NLCs were effectively developed and optimized to improve nose-to-brain delivery. GMS was selected as SL owing to its excellent drug solubilizing capacity and favorable physicochemical stability and stable physical characteristics, while liquid lipid, which Oleic acid has high solubility of drug, was chosen in it. A 70:30 ratio of GMS to oleic acid ensured miscibility and a stable matrix for drug encapsulation. Tween 20 and Pluronic F-68 were selected as surfactant and co-surfactant to ensure particle stability, while *C. crista* seed extract served as a natural mucoadhesive agent. TEM confirmed spherical nanoparticles, and mucoadhesion studies showed strong adhesion, enhancing nasal retention. *In vivo* pharmacokinetic studies revealed significantly higher brain availability of RP through the i.n. compared to i.v. administration.• Overall, RF13 demonstrated efficient drug encapsulation, sustained release, and targeted brain delivery, indicating its strong potential as a promising i.n. delivery for treating PD and other CNS disorders.

AUTHORS' CONTRIBUTIONS

Vidya Thorat: Writing – original draft, methodology, investigation, formal analysis, data curation, and software. Avinash Tekade: Conceptualization, investigation, writing–review & editing, and supervision.

ETHICAL APPROVAL

Institutional Animal Ethics Committee (IAEC) (IAEC Protocol Approval no: IRDI/IAEC/M04/12/2024-25).

DATA AVAILABILITY

The data sets generated during and/or analysed during the current study are available from the corresponding author on reasonable request.

ACKNOWLEDGMENT

The authors would like to acknowledge Marathwada Mitra Mandal's College of Pharmacy, Thergaon (Kalewadi), Pune-411033 (M.S.), India (Affiliated to Savitribai Phule Pune University, Pune), for generously providing the facility and support for carrying out the project.

REFERENCES

1. Pardridge WM. The blood-brain barrier: Bottleneck in brain drug development. NeuroRx 2005;2:3-14.
2. Cilia R, Cereda E, Klersy C, Canesi M, Zecchinelli AL, Tesei S, *et al*. Parkinson's disease beyond 20 years. J Neurol Neurosurg Psychiatry 2014;86:849-55.
3. Deleu D, Northway MG, Hanssens Y. Clinical pharmacokinetic and pharmacodynamic properties of drugs used in the treatment of Parkinson's disease. Clin Pharmacokinet 2002;41:261-309.
4. Tekade AR, Suryavanshi MR, Shewale AB, Patil VS. Design and development of donepezil hydrochloride loaded nanostructured lipid carriers for efficient management of Alzheimer's disease. Drug Dev Ind Pharm 2023;49:590-600.
5. Tomlinson CL, Stowe R, Patel S, Rick C, Gray R, Clarke CE. Systematic review of levodopa dose equivalency reporting in Parkinson's disease. Mov Disord 2010;25:2649-53.
6. Illum L. Nasal drug delivery: New developments and strategies. Drug Discov Today 2002;7:1184-9.
7. Djupesland PG. Nasal drug delivery devices: Characteristics and performance in a clinical perspective-a review. Drug Deliv Transl Res 2013;3:42-62.
8. Tarakad A, Jankovic J. Diagnosis and management of Parkinson's disease. Semin Neurol 2017;37:118-26.
9. Ugwoke MI, Verbeke N, Kinget R. The biopharmaceutical aspects of nasal mucoadhesive drug delivery. J Pharm Pharmacol 2001;53:3-21.
10. Vyas TK, Shahiwala A, Marathe S, Misra A. Intranasal drug delivery for brain targeting. Curr Drug Deliv 2005;2:165-75.
11. Wilson B, Samanta MK, Santhi K, Kumar KP, Ramasamy M, Suresh B. Chitosan nanoparticles as a new delivery system for the anti-Alzheimer drug tacrine. Nanomedicine 2010;6:144-52.
12. Anwar W, Dawaba HM, Afouna MI, Samy AM. Screening study for formulation variables in preparation and characterization of candesartan cilexetil loaded nanostructured lipid carriers. Univ J Pharm Res 2019;4:8-19.
13. Rehman S, Nabi B, Baboota S, Ali J. Tailoring lipid nanoconstructs for the oral delivery of paliperidone: Formulation, optimization and *in vitro* evaluation. Chem Phys Lipids 2021;234:105005.
14. Abascal K, Ganora L, Yarnell E. The effect of freeze-drying and its implications for botanical medicine: A review. Phytother Res 2005;19:655-60.
15. Garg J, Pathania K, Sah SP, Pawar SV. Nanostructured lipid carriers: A promising drug carrier for targeting brain tumours. Fut J Pharm Sci 2022;8:25.
16. Mahor AK, Singh PP, Gupta R, Bhardwaj P, Rathore P, Kishore A, *et al*. Nanostructured lipid carriers for improved delivery of therapeutics via the oral route. J Nanotechnol 2023;2023:4687959.
17. Elmowafy M, Al-Sanea MM. Nanostructured lipid carriers (NLCs) as drug delivery platform: Advances in formulation and delivery strategies. Saudi Pharm J 2021;29:999-1012.
18. Gidwani B, Vyas A, Kaur CD. Cytotoxicity and pharmacokinetics study of nanostructured lipid carriers of mechlorethamine: Preparation, optimization and characterization. Part Sci Technol 2020;38:23-33.
19. Ortiz AC, Yañez O, Salas-Huenuleo E, Morales JO. Development of a nanostructured lipid carrier (NLC) by a low-energy method, comparison of release kinetics and molecular dynamics simulation. Pharmaceutics 2021;13:531.
20. Rajput AP, Butani SB. Resveratrol anchored nanostructured lipid carrier loaded *in situ* gel via nasal route: Formulation, optimization and *in vivo* characterization. J Drug Deliv Sci Technol 2019;51:214-23.
21. Beloqui A, Solinís MA, Rodríguez-Gascón A, Almeida AJ, Préat V. Nanostructured lipid carriers: Promising drug delivery systems for future clinics. Nanomedicine 2016;12:143-61.
22. Rani A, Kaur R, Aldahish A, Vasudevan R, Balaji P, Dora CP, *et al*. Nanostructured lipid carriers (NLC)-based topical formulation of hesperidin for effective treatment of psoriasis. Pharmaceutics 2025;17:478.
23. Mall J, Naseem N, Haider MF, Rahman MA,

Khan S, Siddiqui SN. Nanostructured lipid carriers as a drug delivery system: A comprehensive review with therapeutic applications. Intell Pharm 2024;3:243-55.
24. Khosa A, Reddi S, Saha RN. Nanostructured lipid carriers for site-specific drug delivery. Biomed Pharmacother 2018;103:598-613.
25. Khan S, Sharma A, Jain V. An overview of nanostructured lipid carriers and its application in drug delivery through different routes. Adv Pharm Bull 2022;13:446-60.
26. Teng Z, Yu M, Ding Y, Zhang H, Shen Y, Jiang M, *et al*. Preparation and characterization of nimodipine-loaded nanostructured lipid systems for enhanced solubility and bioavailability. Int J Nanomed 2019;14:119-33.
27. Sudarshan S, Sunil BB. *In vivo* mucoadhesive strength appraisal of gum *Manilkara zapota*. Braz J Pharm Sci 2015;51:689-98.
28. Mohanty D, Alsaidan OA, Zafar A, Dodle T, Gupta JK, Yasir M, *et al*. Development of atomoxetine-loaded NLC *in situ* gel for nose-to-brain delivery: Optimization, *in vitro*, and preclinical evaluation. Pharmaceutics 2023;15:1985.
29. Sathyanarayana T, Sudheer P, Jacob E, Sabu MM. Development and evaluation of nanostructured lipid carriers for transdermal delivery of ketoprofen. Fabad J Pharm Sci 2023;48:105-24.
30. Devkar TB, Tekade AR, Khandelwal KR. Surface engineered nanostructured lipid carriers for efficient nose to brain delivery of ondansetron HCl using *Delonix regia gum* as a natural mucoadhesive polymer. Colloids Surf B Biointerfaces 2014;122:143-50.
31. Ahmed S, Mahmood S, Ansari MD, Gull A, Sharma N, Sultana Y. Nanostructured lipid carrier to overcome Stratum corneum barrier for the delivery of agomelatine in rat brain; Formula optimization, characterization and brain distribution study. Int J Pharm 2021;607:121006.
32. Abdelmonem RE, El-Nabarawi MA, Attia AM, Teaimaa MA. Ocular delivery of natamycin solid lipid nanoparticle loaded mucoadhesive gel: Formulation, characterization and *in vivo* study. Int J Appl Pharm 2020;12:173-80.
33. Zhang DR, Li ZY, Feng FF, Wang YC, Dai WT, Zhang Q, *et al*. Preparation and characterization of silybin-loaded nanostructured lipid carriers. Drug Deliv 2010;17:11-8.
34. Dhasade VV, Komala M. Phytochemical analysis and antitubercular potential of *Pimenta dioica* Linn. Neuroquantology 2022;20:6951-61.

Source of Support: Nil. **Conflicts of Interest:** None declared.